**Supplemental Figure 1. Blockade of MAPK signaling reduced basal levels of CCS-*lacZ* expression.** (A) Representative E9.5 X-gal stained CCS-*lacZ* hearts treated with vehicle control for 24 or 48hrs. Images presented in Figure 1A. (B) Representative E9.5 X-gal stained CCS-*lacZ* hearts cultured with kinase inhibitors for 24 or 48hrs. (C) Schematic representation of NRG1-ErbB2/ErbB4 intracellular signaling highlighting pathway specific kinase inhibitors. Doses used for kinase inhibitor studies were: PP2 (10uM), LY294002 (25µM), PD98059 (50µM), FR180204 (20µM), SL0101 (50µM), H89 (10µM). Outflow flow tract (OFT). Scale: 200µm (A,B).
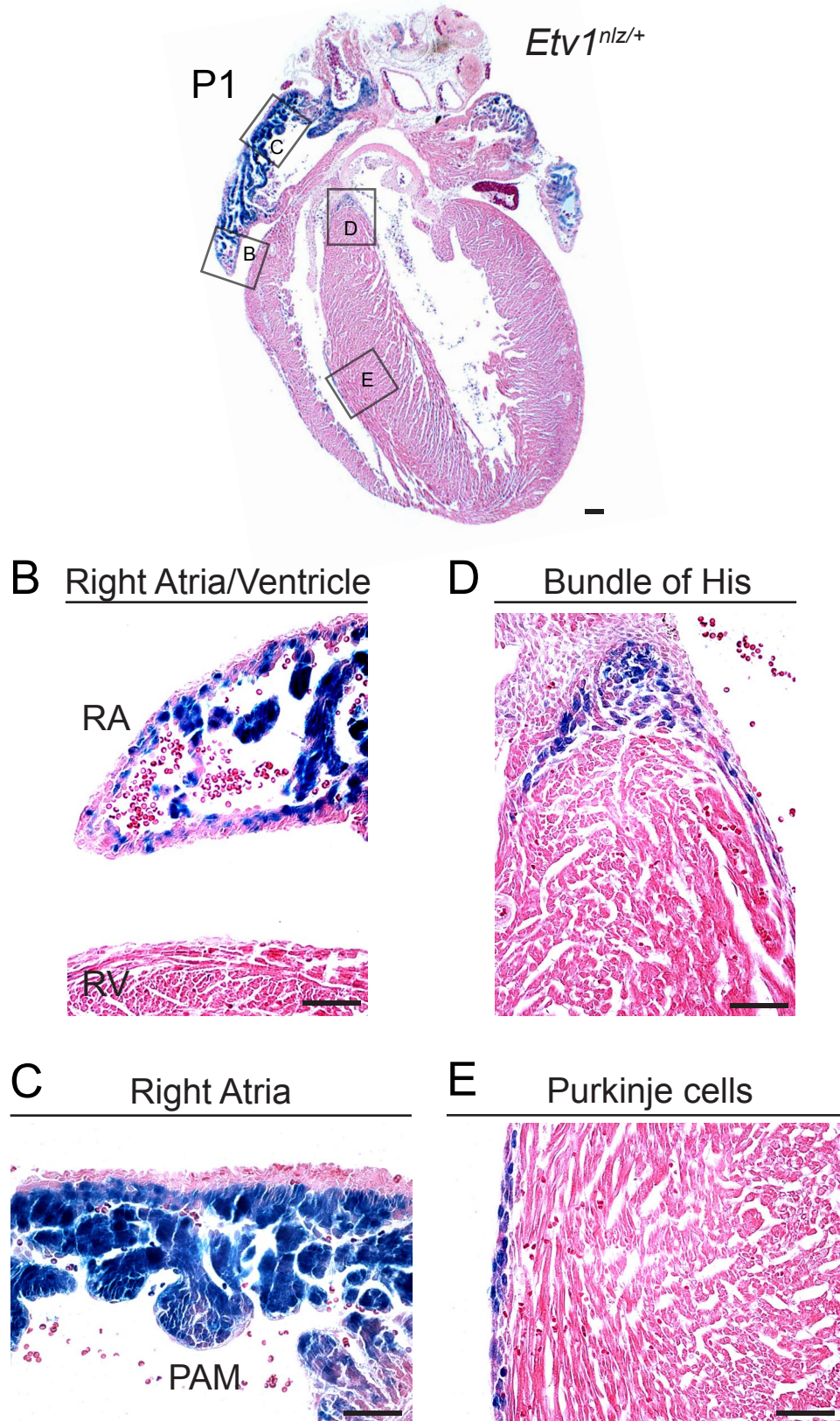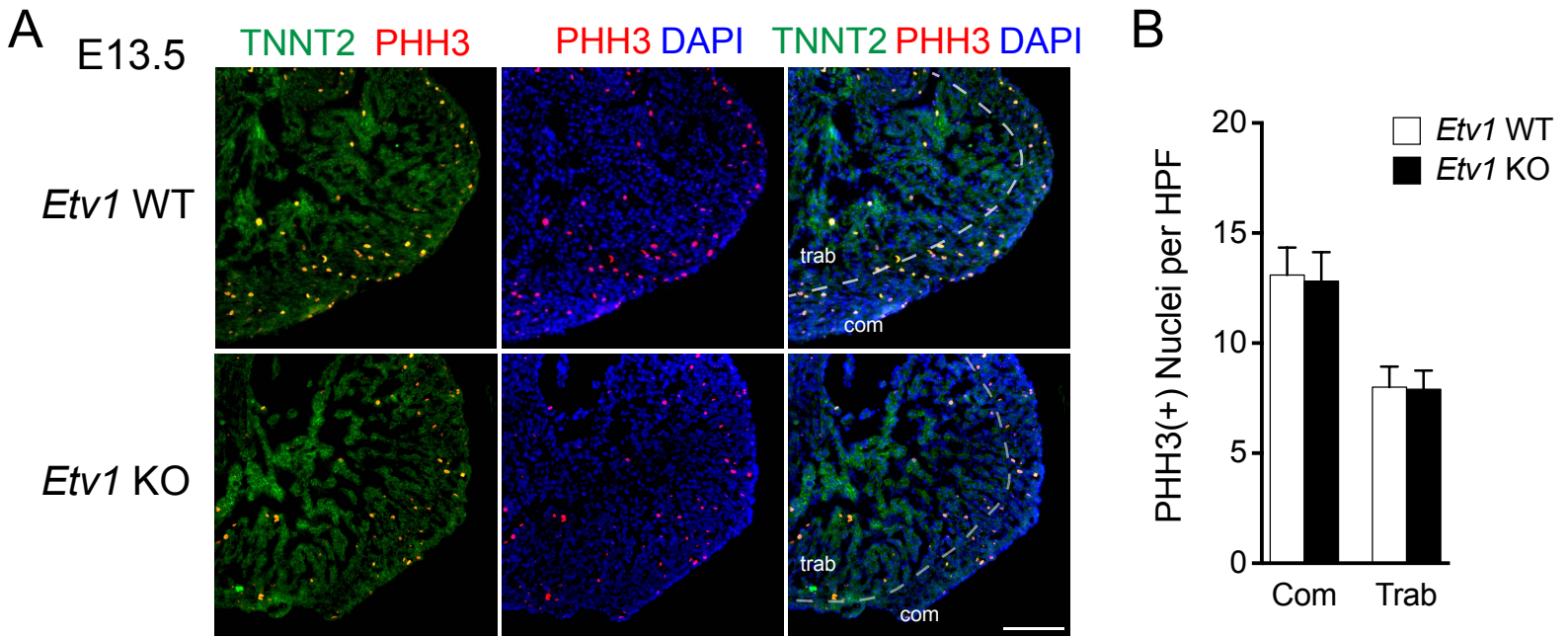
Supplemental Figure 2. *Etv1* expression in the postnatal mouse heart. (A) X-gal and eosin stained P1 *Etv1*^{nlz/+} heart. High magnification regions of Etv1-nlz expression shown: (B,C) Right atria (RA), (D) Bundle of His, and (E) Purkinje cells. *Etv1* expression was identified via X-gal positive staining (blue). Eosin counterstain enabled visualization of cardiac structures (pink). Right ventricle (RV), Pectinated atrial myocardium (PAM). Scale: 100μm(A); 50μm (B-E).
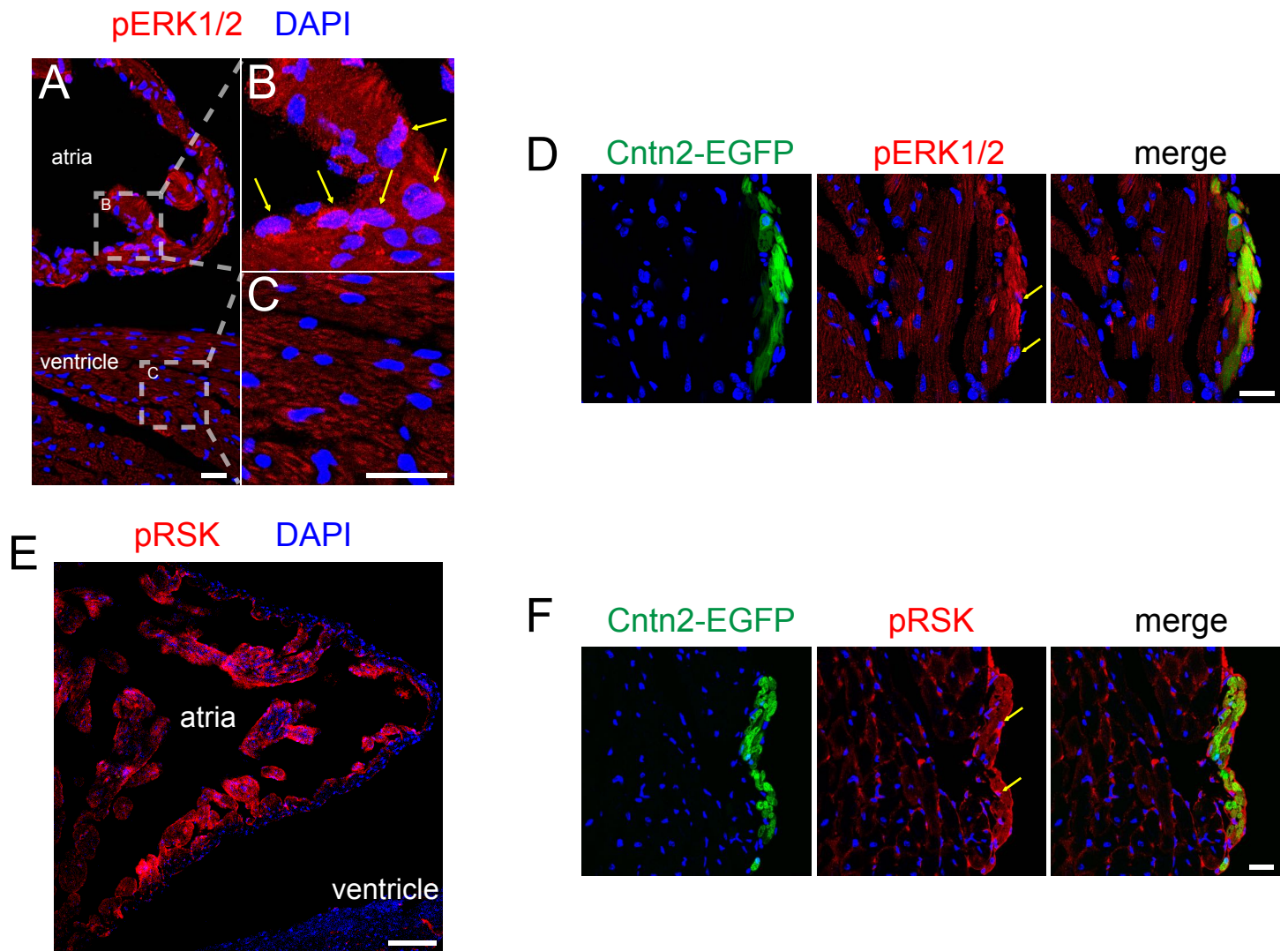
Supplemental Figure 3. pERK1/2 / pRSK signaling remains active in postnatal atrial and Purkinje myocytes. (A-D) Immunofluorescence staining of pERK1/2 in P21 *Cntn2EGFP/+* hearts. (A) Low magnification view of atrial and ventricular regions. High magnification of pErk1/2 expression: (B) Atria, (C) ventricle, and (D) Purkinje regions. (E-F) Immunofluorescence staining of pRSK in P21 *Cntn2EGFP/+* hearts: (E) Atria and (F) Purkinje regions. Nuclei were stained with DAPI, pERK1/2-red (A-D), pRSK-red (E-F), and CNTN2-EG-FP-green). Yellow arrows identify representative regions of nuclear expression. Scale: 25μm(A-D, F); 100μm (E).
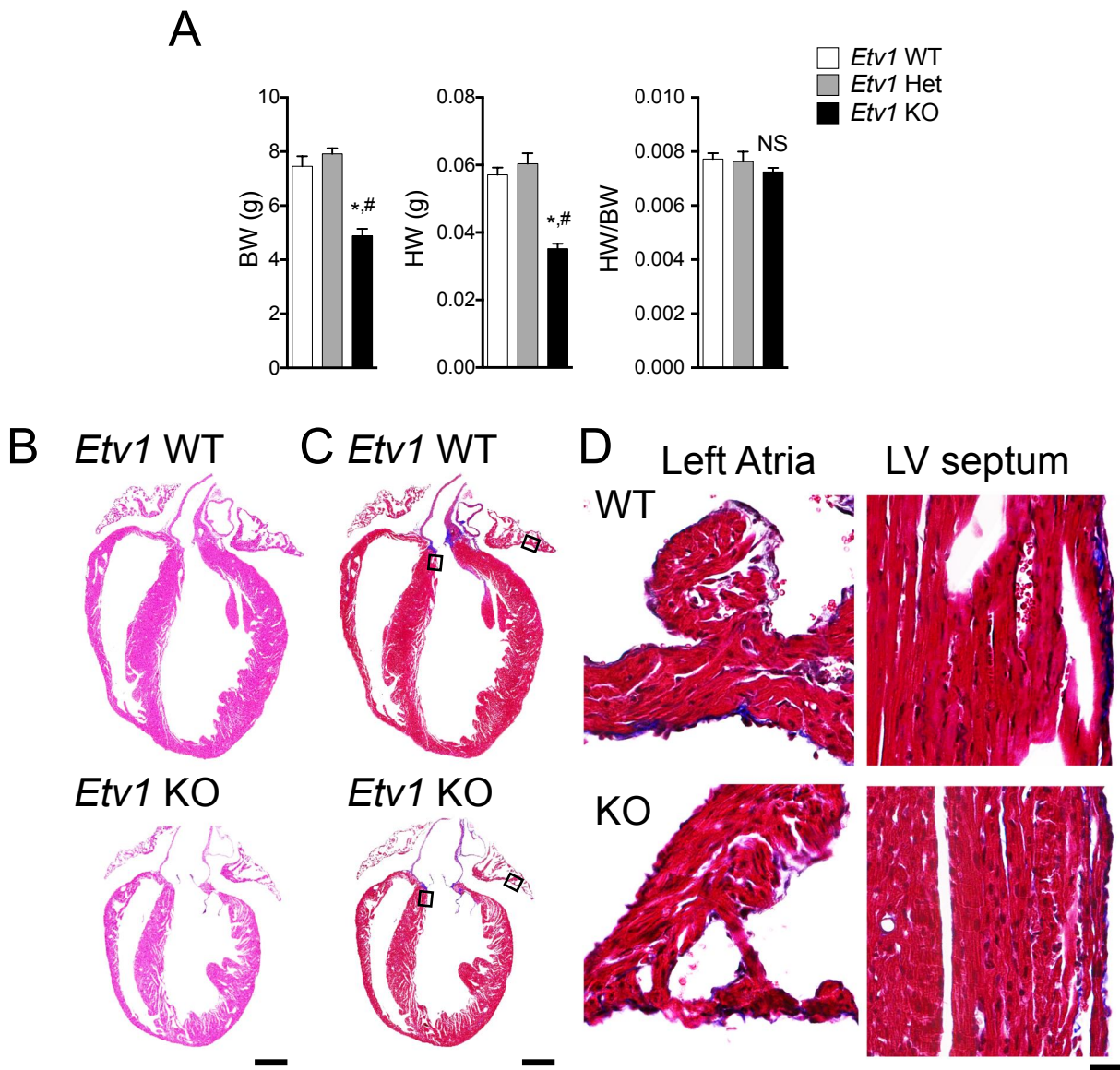
Supplemental Figure 4. Cardiac structural and functional assessment of *Etv1* WT, Het, and KO mice. (A) Heart weight (HW), Body weight (BW), and HW/BW ratios of *Etv1* WT, Het, and KO mice. (B) Hematoxylin and eosin and (C) trichrome stain of *Etv1* WT and KO hearts. (D) High magnification view of black boxed regions in the left atria and ventricle of trichrome stained samples (from C). Left Ventricle (LV), Not significant (NS). Data represent mean ± SEM. *P<0.05 KO vs WT, #P<0.05 KO vs Het, one-way ANOVA. Scale: 500µm (B and C), 50µm (D).

Supplemental Figure 5. Cell cycling is unperturbed in *Etv1* null hearts. (A) Phospho-Histone H3 (PHH3) expression (red) was evaluated by immunofluorescence in *Etv1* WT and KO left ventricular regions at E13.5. Cardiomyocytes were identified with cardiac troponin T (TNNT2) (green). (B) The number of mitotic cells in the compact and trabecular myocardium was quantified per high power field (HPF, 40x). (n=20 HPF from n=3 hearts). Data represent mean ± SEM. Nuclei were stained with DAPI (blue). Trabecular myocytes (trab), Compact zone myocytes (com). Scale: 25µm (A).
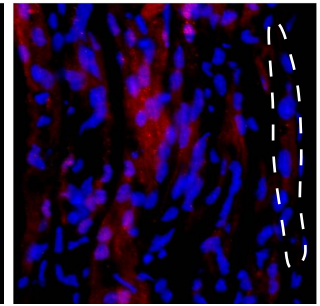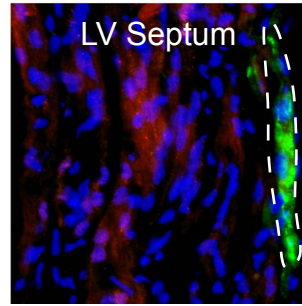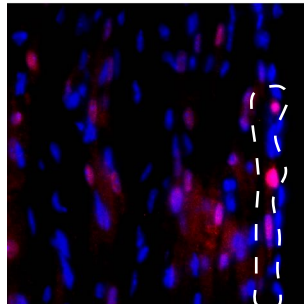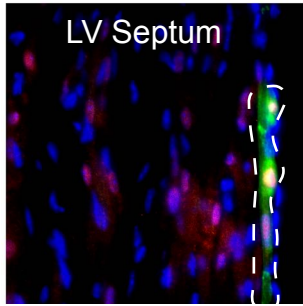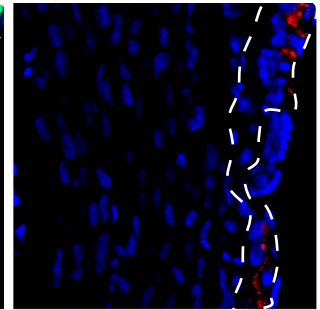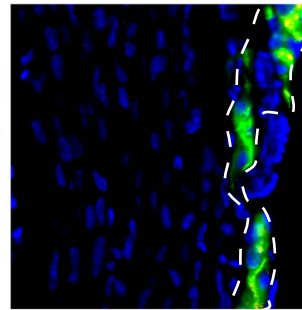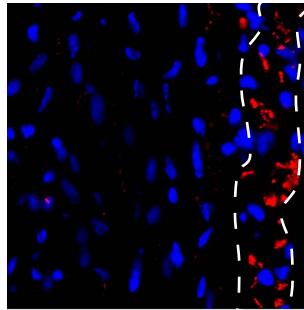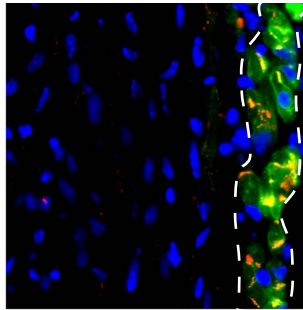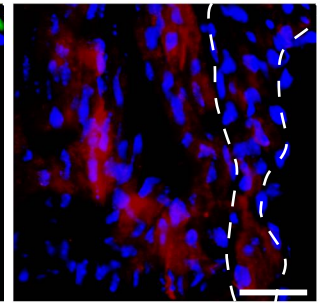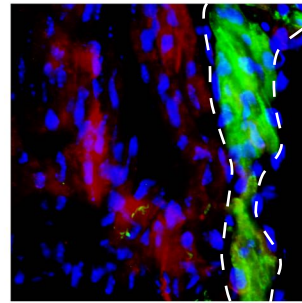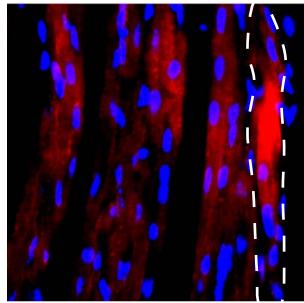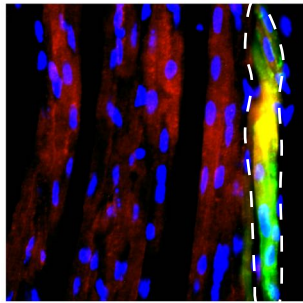
Supplemental Figure 6. Decreased NKX2-5, Cx40 and Na$_V$1.5 expression in Purkinje cells from P18 *Etv1* KO hearts. NKX2-5, Cx40, and Na$_V$1.5 expression (red) was evaluated by immunofluorescence in P18 *Etv1* WT and KO heart sections. Purkinje cells were identified by CNTN2 expression (green). Nuclei were stained with DAPI (blue). Dotted lines outline CNTN2+ Purkinje cells. Left ventricle (LV). Scale: 50μm.
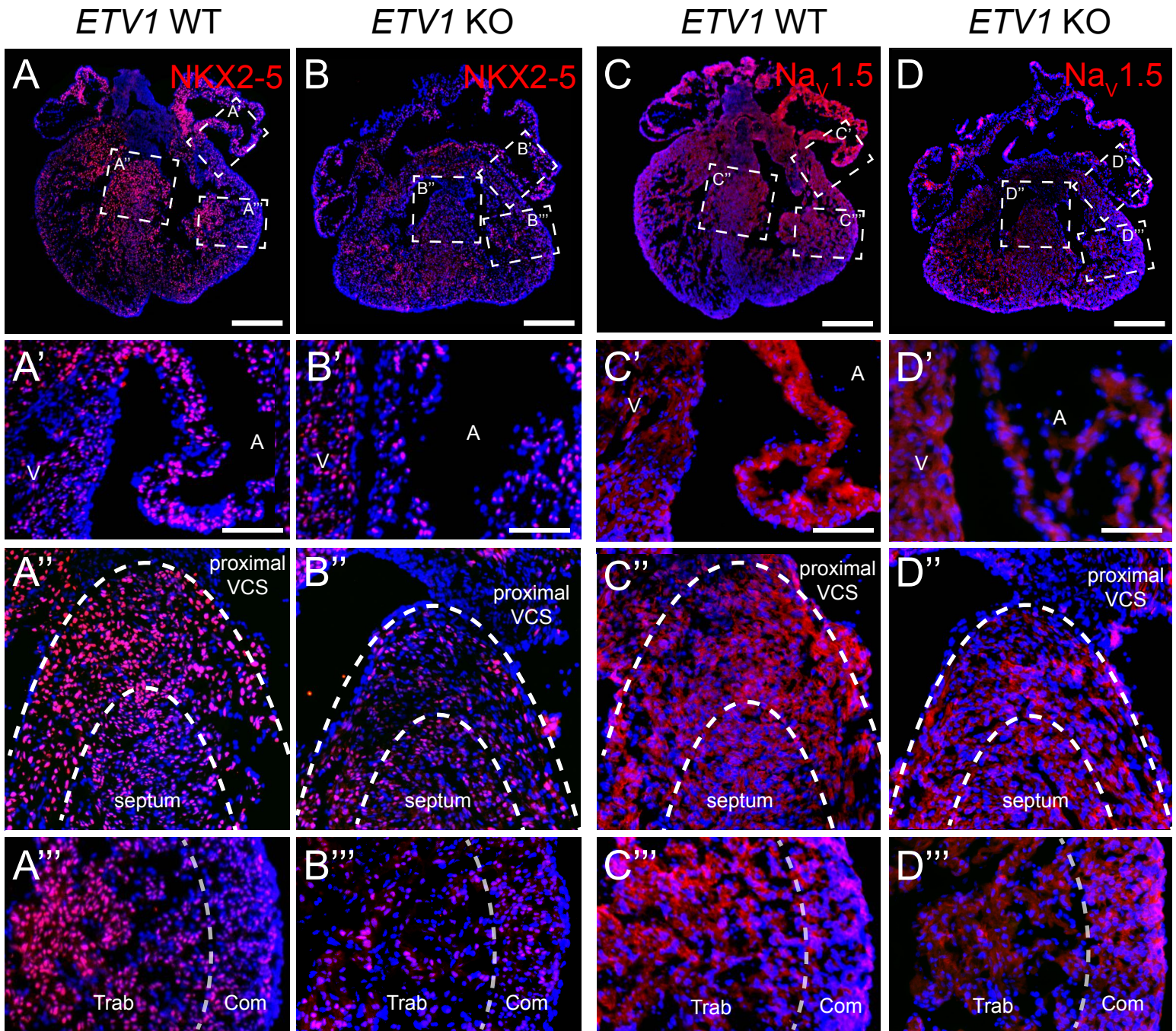
Supplemental Figure 7. E13.5 *Etv1* KO hearts display reduced levels of NKX2-5 and Na$_V$1.5 in the atria, proximal VCS, and trabecular myocardium. (A-B) NKX2-5 and (C-D) Na$_V$1.5 expression (red) was evaluated by immunofluorescence in E13.5 *Etv1* WT and KO hearts. High magnification views of boxed regions comparing atrium (A) vs ventricle (V) (A'-D'), proximal ventricular conduction system (VCS) vs ventricular septum (A''-D''), and trabecular (Trab) myocardium vs compact (Com) myocardium (A'''-D'''). Nuclei were stained with DAPI (blue). Scale: 50µm (A-D), 25µm (A'-'''-D'-''').
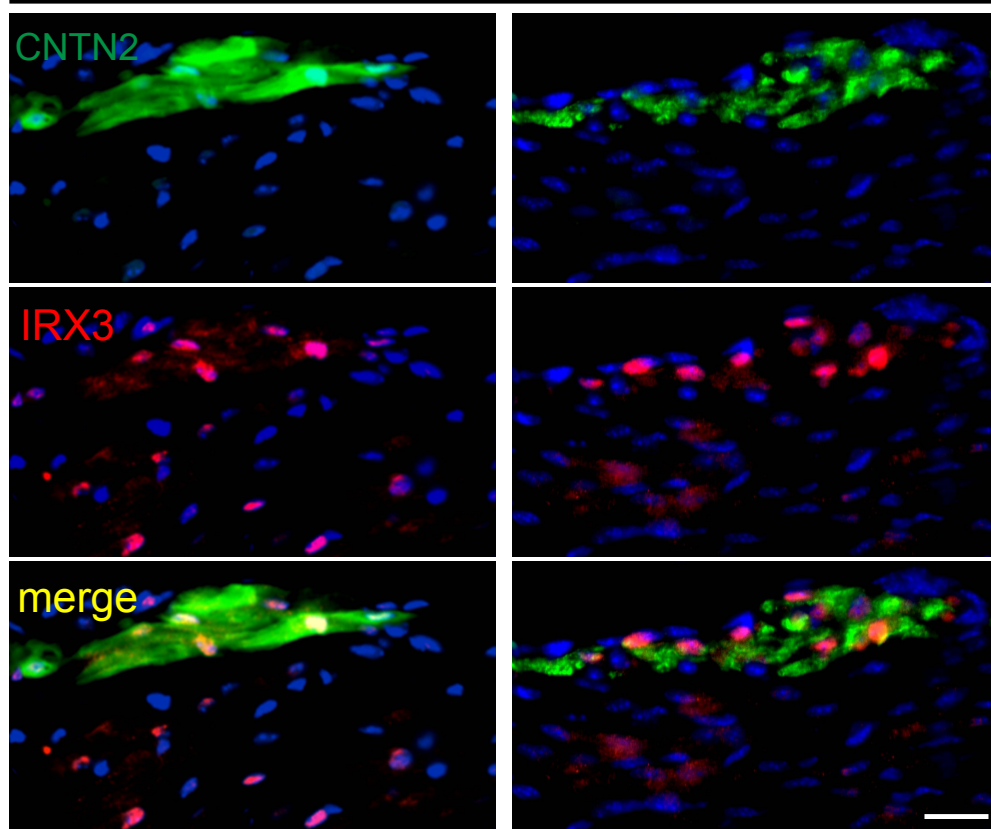
Supplemental Figure 8. IRX3 expression is preserved in *Etv1* null hearts. IRX3 expression (red) was evaluated by immunofluorescence in P18 *Etv1* WT and KO heart sections. Purkinje cells were identified by CNTN2 expression (green). Nuclei were stained with DAPI (blue). Scale: 20μm.
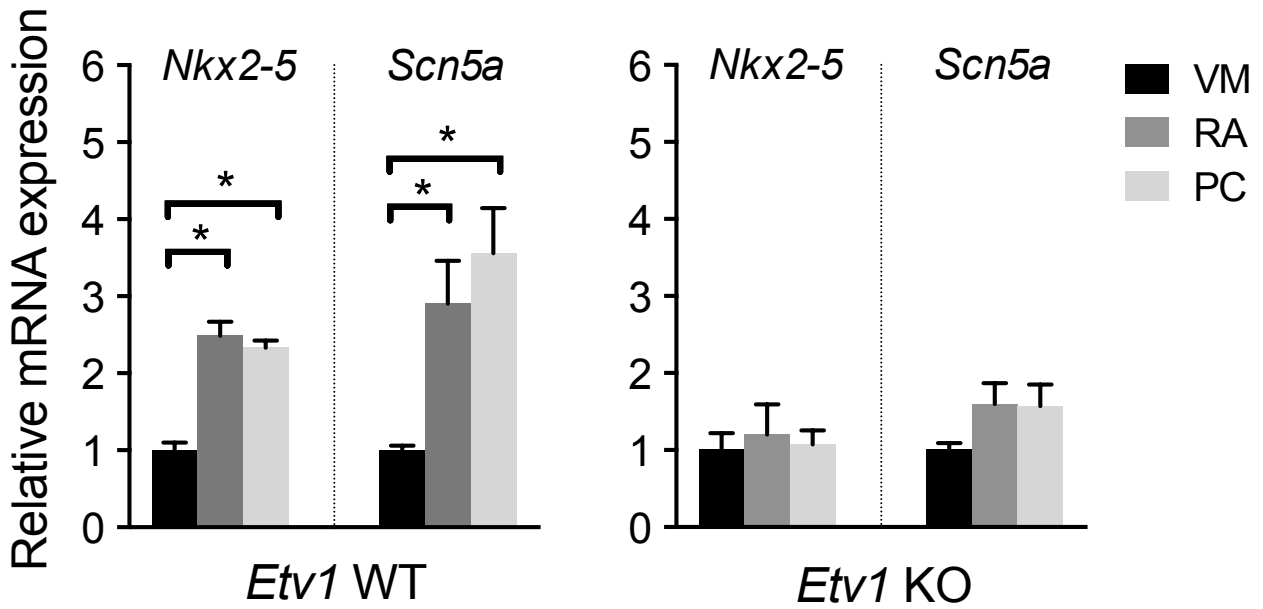
Supplemental Figure 9. *Nkx2-5* and *Scn5a* transcript levels from FACS purified atrial and Purkinje *Etv1* KO myocytes are reduced to ventricular levels. Quantitative RT-PCR of *Nkx2-5* and *Scn5a* transcript levels (normalized to *GAPDH*) in P18 isolated cardiac cells, displayed relative to ventricular myocytes. Ventricular myocytes (VM), Right Atria (RA), Purkinje cells (PC). Data represent mean ± SEM. *$P < 0.05$, one-way ANOVA.
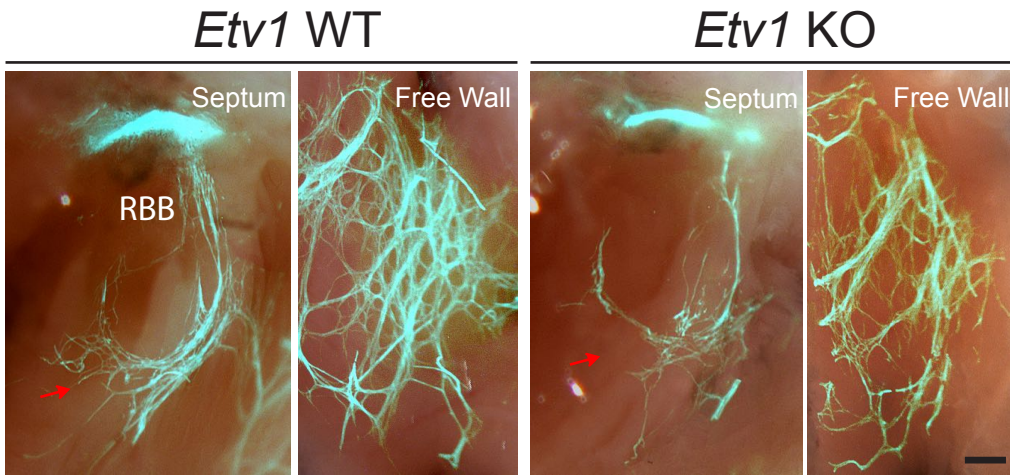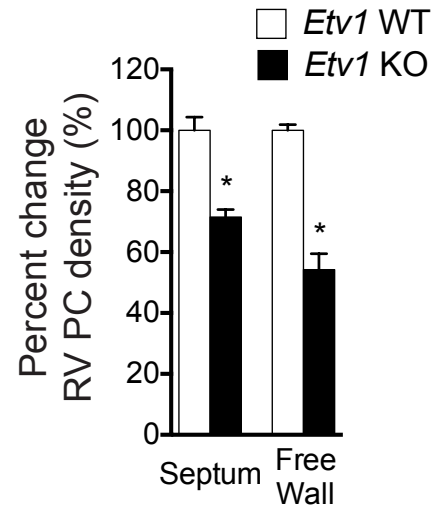
Supplemental Figure 10. *Etv1* KO hearts exhibit hypoplasia of the right VCS. (A) The right ventricular (RV) conduction system (septum and free wall) was visualized in P18 *Etv1* WT and KO hearts backcrossed into the *Cntn2*^{EGFP/+} reporter line. P18 *Etv1* KO/Cntn2^{EGFP/+} hearts displayed hypoplasia of the right PC network compared to *Etv1* WT/*Cntn2*^{EGFP/+} control hearts (red arrows). (B) Percentage of PC (Cntn2^{EGFP}+) area was significantly reduced on the RV septum and free wall in *Etv1* null hearts (n=3). Right bundle branch (RBB). Data represent mean ± SEM. *P<0.05, two-tailed Student's t-test. Scale: 500μm.
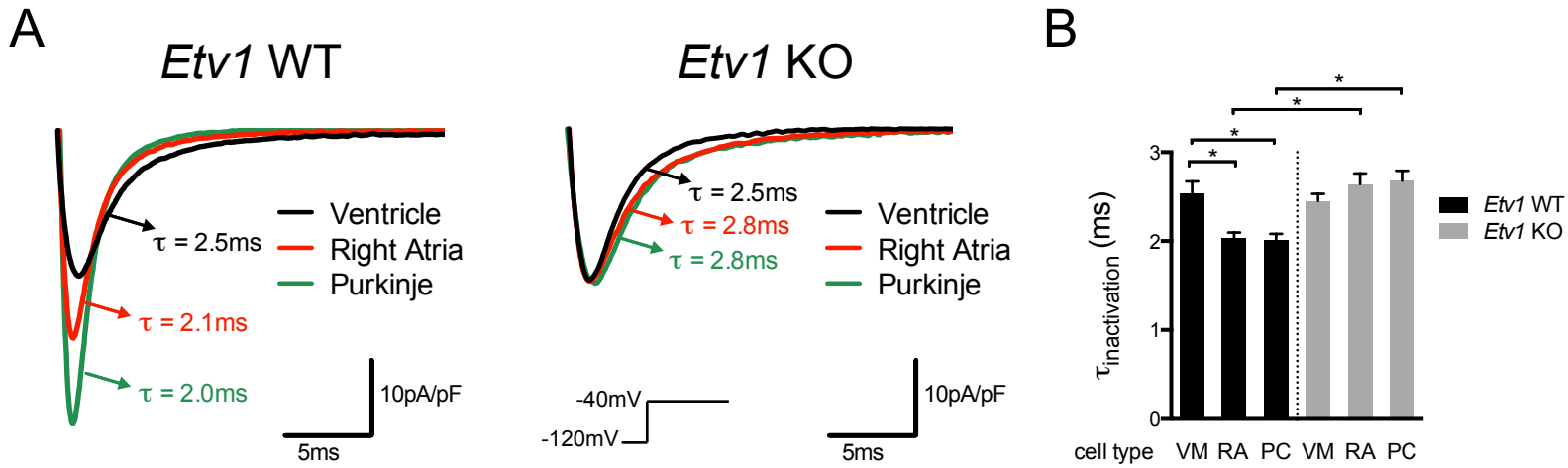
Supplemental Figure 11. Sodium current traces and time-dependent inactivation in *Etv1* WT and KO myocytes. Whole-cell patch clamp was performed on dissociated cardiac cells (ventricular, right atrial, Purkinje myocytes) from P18 *Etv1* WT and KO mice in a *Cntn2*^EGFP/+^ background. (A) Superimposed representative sodium current traces from *Etv1* WT and KO cells following depolarization to −40 mV. The time course of inactivation was fit with a single exponential function. Representative time constant (τ) of inactivation are shown. (B) Time constants plotted for *Etv1* WT and KO ventricular (VM), right atria (RA), and Purkinje cells (PC) (n=4). Data represent mean ± SEM. *P<0.05, one-way ANOVA.

Supplemental Table 1: Surface and intracardiac electrograms (IEGM) were obtained in mice at P18 of age. Numbers in parentheses indicate the number of mice recorded for surface and intracardiac ECG values, respectively. HR; Heart rate; AH, atrial-His; HV, His-ventricular; AVI, Atrioventricular interval. Not significant (NS). Data represents mean ± SEM.

Cardiac conduction intervals in P18 *Etv1* WT, Het, and KO mice

	ECG						IEGM			
	HR (bpm)	PR (ms)	P (ms)	QRS (ms)	JT (ms)	RsR'	HR (bpm)	AH (bpm)	HV (ms)	AVI (ms)
WT (10,6)	425 ± 15	31.8 ± 0.7	13.7 ± 0.4	11.3 ± 0.2	6.0 ± 0.5	0%	576 ± 30	20.3 ± 0.9	7.2 ± 0.4	27.5 ± 1.2
Het (10,5)	451 ± 10	30.0 ± 1.0	14.5 ± 0.5	11.1 ± 0.2	6.4 ± 0.1	0%	543 ± 20	21.7 ± 0.9	7.7 ± 0.3	29.4 ± 1.1
KO (10,5)	419 ± 25	43.3 ± 2.0	20.8 ± 0.5	14.7 ± 0.3	8.0 ± 0.9	30%	566 ± 49	26.4 ± 1.7	9.4 ± 0.4	36.6 ± 1.6
P values										
WT vs Het	NS	NS	NS	NS	NS	-	NS	NS	NS	NS
Het vs KO	NS	< 0.0001	< 0.0001	< 0.0001	NS	-	NS	0.04	0.01	0.01
WT vs KO	NS	< 0.0001	< 0.0001	< 0.0001	NS	-	NS	0.01	0.002	0.002

Supplemental Table 2: Left ventricular cardiac function and wall thickness were obtained in mice at P18 of age via echocardiography. Numbers in parentheses indicate the number of mice recorded. SV, stroke volume; EF, ejection fraction; LV, left ventricle; AW, anterior wall; PW, posterior wall; d, diastole; s, systole. Not significant (NS). Data represents mean ± SEM.

Echocardiographic parameters in P18 *Etv1* WT, Het, and KO mice

	SV (ul)	EF (%)	LVAW,s (mm)	LVAW,d (mm)	LVPW,s (mm)	LVPW,d (mm)
WT (10)	18.4 +/- 2.3	56.4 +/- 3.7	0.55 +/- 0.03	1.09 +/- 0.02	0.54 +/- 0.04	1.03 +/- 0.03
Het (10)	17.7 +/- 1.3	58.7 +/- 3.2	0.57 +/- 0.05	1.04 +/- 0.02	0.59 +/- 0.03	1.01 +/- 0.01
KO (10)	15.0 +/- 0.3	67.9 +/- 2.5	0.54 +/- 0.02	1.00 +/- 0.04	0.56 +/- 0.02	0.97 +/- 0.03
P values						
WT vs Het	NS	NS	NS	NS	NS	NS
Het vs KO	NS	< 0.05	NS	NS	NS	NS
WT vs KO	NS	< 0.05	NS	NS	NS	NS

Supplemental Table 3: Relative levels of NKX2-5, Cx40, and Na$_V$1.5 in atrial myocytes from *Etv1* WT, Het, and KO hearts. Western blot densitometry quantification of protein levels (normalized to Vinculin), presented relative to WT.

	Nkx2-5	Cx40	Na$_V$1.5
Etv1 WT (n=6)	1.00 ± 0.03	1.00 ± 0.05	1.00 ± 0.07
Etv1 Het (n=6)	1.11 ± 0.10	1.09 ± 0.10	1.03 ± 0.08
Etv1 KO (n=6)	0.55 ± 0.05*	0.50 ± 0.08*	0.64 ± 0.07*

*P<0.05 vs WT or Het

Supplemental Table 4: Relative levels of *Nkx2-5*, *Gja5*, *Scn5a,* and *Tbx5* in FACS purified ventricular, atrial, and Purkinje myocytes from *Etv1* WT and KO hearts. Quantitative RT-PCR of transcript levels (normalized to GAPDH), presented relative to WT.

	Nkx2-5	*Gja5*	*Scn5a*	*Tbx5*
VM *Etv1* WT (n=4)	1.00 ± 0.17	-	1.00 ± 0.03	1.00 ± 0.06
VM *Etv1* KO (n=4)	0.93 ± 0.17	-	0.84 ± 0.13	1.13 ± 0.04
RA *Etv1* WT (n=4)	1.00 ± 0.03	1.00 ± 0.02	1.00 ± 0.07	1.00 ± 0.03
RA *Etv1* KO (n=4)	0.50 ± 0.12*	0.56 ± 0.10*	0.63 ± 0.03*	1.43 ± 0.07*
PC *Etv1* WT (n=4)	1.00 ± 0.10	1.00 ± 0.10	1.00 ± 0.03	1.00 ± 0.07
PC *Etv1* KO (n=4)	0.47 ± 0.07*	0.60 ± 0.04*	0.55 ± 0.06*	1.53 ± 0.07*

*P<0.05 vs WT

Supplemental Table 5: Sodium channel biophysical properties between ventricular, atrial, and Purkinje myocytes from *Etv1* WT and KO hearts.

	Etv1 WT (N=4 mice)			*Etv1* KO (N=4 mice)		
	VM	RA	PC	VM	RA	PC
Maximum Conductance (nS/pF)	0.61 ± 0.03 (n=10)	0.78 ± 0.03 (n=10)	1.11 ± 0.09 (n=13)	0.65 ± 0.03 (n=10)	0.59 ± 0.03 (n=16)	0.61 ± 0.06 (n=12)
$V_{0.5}$, activation (mV)	-47.2 ± 1.1 (n=10)	-57.8 ± 1.4 (n=10)	-57.7 ± 1.6 (n=13)	-48.3 ± 0.7 (n=10)	-46.6 ± 1.1 (n=16)	-50.9 ± 2.1 (n=12)
$V_{0.5}$, inactivation (mV)	-80.0 ± 1.3 (n=10)	-86.8 ± 1.2 (n=9)	-80.2 ± 0.8 (n=11)	-82.0 ± 1.3 (n=10)	-80.2 ± 1.1 (n=16)	-77.9 ± 2.8 (n=8)
Tau of recovery from inactivation (ms)	3.2 ± 0.4 (n=10)	6.5 ± 1.0 (n=9)	5.7 ± 0.3 (n=11)	3.6 ± 0.2 (n=10)	3.4 ± 0.2 (n=16)	2.9 ± 0.2 (n=8)
Tau of inactivation (ms)	2.5 ± 0.1 (n=10)	2.0 ± 0.1 (n=10)	2.0 ± 0.1 (n=13)	2.5 ± 0.1 (n=10)	2.6 ± 0.1 (n=16)	2.7 ± 0.1 (n=12)

*Statistics outlined in supplementary tables 6-10

Supplemental Table 6: One-way ANOVA of sodium channel maximum conductance (nS/pF)

One-way ANOVA Max. Conductance (nS/pF)	Mean Diff.	90% CI of diff.	Summary	P Value
Etv1 WT VM vs. *Etv1* WT RA	-0.1687	-0.3063 to -0.03118	*	0.0447
Etv1 WT VM vs. *Etv1* WT PC	-0.4991	-0.6285 to -0.3697	****	< 0.0001
Etv1 WT VM vs. *Etv1* KO VM	-0.03141	-0.1690 to 0.1062	ns	0.7044
Etv1 WT RA vs. *Etv1* KO RA	0.1892	0.06366 to 0.3148	*	0.0144
Etv1 WT RA vs. *Etv1* KO PC	0.1700	0.03829 to 0.3017	*	0.0350
Etv1 WT PC vs. *Etv1* KO PC	0.5003	0.3772 to 0.6235	****	< 0.0001
Etv1 KO VM vs. *Etv1* KO RA	0.05189	-0.07369 to 0.1775	ns	0.4929
Etv1 KO VM vs. *Etv1* KO PC	0.03266	-0.09905 to 0.1644	ns	0.6804
Etv1 KO RA vs. *Etv1* KO PC	-0.01924	-0.1384 to 0.09990	ns	0.7884

Supplemental Table 7: One-way ANOVA of sodium channel $V_{0.5}$, activation (mV)

One-way ANOVA $V_{0.5}$, activation (mV)	Mean Diff.	95% CI of diff.	Summary	P Value
Etv1 WT VM vs. *Etv1* WT RA	10.88	6.695 to 15.07	****	< 0.0001
Etv1 WT VM vs. *Etv1* WT PC	11.18	7.240 to 15.12	****	< 0.0001
Etv1 WT VM vs. *Etv1* KO VM	1.294	-2.892 to 5.481	ns	0.5392
Etv1 WT RA vs. *Etv1* WT PC	0.2959	-3.642 to 4.234	ns	0.8812
Etv1 WT RA vs. *Etv1* KO RA	-10.97	-14.70 to -7.238	****	< 0.0001
Etv1 WT PC vs. *Etv1* KO PC	-7.078	-10.83 to -3.330	***	0.0004
Etv1 KO VM vs. *Etv1* KO RA	-1.381	-5.112 to 2.350	ns	0.4624
Etv1 KO VM vs. *Etv1* KO PC	2.805	-1.204 to 6.814	ns	0.1671
Etv1 KO RA vs. *Etv1* KO PC	4.186	0.6565 to 7.716	*	0.0208

Supplemental Table 8: One-way ANOVA of sodium channel $V_{0.5}$, inactivation (mV)

One-way ANOVA $V_{0.5}$, inactivation (mV)	Mean Diff.	90% CI of diff.	Summary	P Value
Etv1 WT VM vs. *Etv1* WT RA	6.820	3.302 to 10.34	**	0.0020
Etv1 WT VM vs. *Etv1* WT PC	0.2101	-3.136 to 3.556	ns	0.9168
Etv1 WT VM vs. *Etv1* KO VM	2.035	-1.390 to 5.460	ns	0.3248
Etv1 WT RA vs. *Etv1* WT PC	-6.610	-10.05 to -3.168	**	0.0022
Etv1 WT RA vs. *Etv1* KO RA	-6.574	-9.731 to -3.417	***	0.0009
Etv1 WT PC vs. *Etv1* KO PC	-2.291	-5.850 to 1.267	ns	0.2863
Etv1 KO VM vs. *Etv1* KO RA	-1.788	-4.840 to 1.263	ns	0.3314
Etv1 KO VM vs. *Etv1* KO PC	-4.116	-7.749 to -0.4836	ns	0.0632
Etv1 KO RA vs. *Etv1* KO PC	-2.328	-5.611 to 0.9557	ns	0.2409

Supplemental Table 9: One-way ANOVA of sodium channel Tau of recovery from inactivation (ms)

One-way ANOVA Tau of recovery from inactivation (ms)	Mean Diff.	90% CI of diff.	Summary	P Value
Etv1 WT VM vs. *Etv1* WT RA	-3.326	-4.587 to -2.065	****	< 0.0001
Etv1 WT VM vs. *Etv1* WT PC	-2.541	-3.802 to -1.280	**	0.0014
Etv1 WT VM vs. *Etv1* KO VM	-0.4103	-1.671 to 0.8507	ns	0.5881
Etv1 WT RA vs. *Etv1* WT PC	0.7853	-0.4036 to 1.974	ns	0.2738
Etv1 WT RA vs. *Etv1* KO RA	3.135	1.996 to 4.273	****	< 0.0001
Etv1 WT PC vs. *Etv1* KO PC	2.795	1.534 to 4.056	***	0.0005
Etv1 KO VM vs. *Etv1* KO RA	0.2191	-0.9193 to 1.357	ns	0.7485
Etv1 KO VM vs. *Etv1* KO PC	0.6647	-0.5964 to 1.926	ns	0.3815
Etv1 KO RA vs. *Etv1* KO PC	0.4456	-0.7679 to 1.659	ns	0.5412

Supplemental Table 10: One-way ANOVA of sodium channel Tau of inactivation (ms)

One-way ANOVA Tau of inactivation (ms)	Mean Diff.	90% CI of diff.	Summary	P Value
Etv1 WT VM vs. *Etv1* WT RA	0.4960	0.04210 to 0.9499	*	0.0027
Etv1 WT VM vs. *Etv1* WT PC	0.5202	0.09325 to 0.9471	**	0.0009
Etv1 WT VM vs. *Etv1* KO VM	0.08289	-0.3834 to 0.5492	ns	0.6125
Etv1 WT RA vs. *Etv1* WT PC	0.02415	-0.4028 to 0.4511	ns	0.8718
Etv1 WT RA vs. *Etv1* KO RA	-0.6020	-1.016 to -0.1877	***	< 0.0001
Etv1 WT PC vs. *Etv1* KO PC	-0.6662	-1.072 to -0.2599	***	< 0.0001
Etv1 KO VM vs. *Etv1* KO RA	-0.1889	-0.6168 to 0.2390	ns	0.2109
Etv1 KO VM vs. *Etv1* KO PC	-0.2289	-0.6764 to 0.2187	ns	0.1480
Etv1 KO RA vs. *Etv1* KO PC	-0.04000	-0.4331 to 0.3531	ns	0.7717

Supplemental Table 11: PheWAS results for *ETV1* rs9639168 in African Americans. All phenotypes with p<0.01 are reported below.

Phenotype	Cases	Controls	Odds ratio (95% CI)	p
Bundle branch block	56	2530	2.13 (1.40 - 3.22)	0.00037
Left bundle branch block	34	2530	2.53 (1.50 - 4.26)	0.00046
Malignant neoplasm of ovary and other uterine adnexa	36	3487	2.22 (1.36 - 3.64)	0.00152
Malignant neoplasm of ovary	27	3487	2.42 (1.38 - 4.24)	0.00200
Sepsis and SIRS	276	3875	0.69 (0.54 - 0.89)	0.00368
Sepsis	252	3875	0.69 (0.53 - 0.89)	0.00480
Cancer of other female genital organs	53	3487	1.84 (1.20 - 2.80)	0.00490
Conduction disorders	67	3844	1.72 (1.18 - 2.51)	0.00518
Lack of coordination	80	3777	1.64 (1.16 - 2.32)	0.00539
Psychosis	60	2858	1.76 (1.18 - 2.63)	0.00577
Pancreatic cancer	26	4011	2.23 (1.25 - 3.97)	0.00677

Supplemental Table 12: PheWAS results for *ETV1* rs9639168 in European Americans. All phenotypes with p<0.01 are reported below.

Phenotype	Cases	Controls	Odds ratio (95% CI)	p
Other heart block	24	17611	2.85 (1.60 - 5.06)	0.00036
Stricture/obstruction of ureter	239	21792	1.34 (1.11 - 1.60)	0.00197
Premature menopause and other ovarian failure	71	24530	1.63 (1.17 - 2.26)	0.00373
Abnormal results of other function studies (bladder, pancreas, placenta, spleen, etc)	25	29519	2.26 (1.30 - 3.94)	0.00396
Inflammation of the eye	1243	25181	0.88 (0.81 - 0.96)	0.00482
Primary/intrinsic cardiomyopathies	1116	26859	0.88 (0.80 - 0.96)	0.00499
Hereditary and idiopathic peripheral neuropathy	1167	26375	0.88 (0.80 - 0.96)	0.00499
Hypertension complicating pregnancy, childbirth, and the puerperium	192	29396	0.73 (0.58 - 0.91)	0.00522
Conjunctivitis, noninfectious	527	25181	0.83 (0.72 - 0.95)	0.00539
Other specified nonpsychotic and/or transient mental disorders	1377	23431	0.89 (0.82 - 0.97)	0.00592
Microscopic hematuria	179	20671	0.73 (0.58 - 0.92)	0.00706
Other benign neoplasm of connective and other soft tissue	74	28408	1.55 (1.12 - 2.15)	0.00756
Polyp of corpus uteri	104	29059	1.45 (1.10 - 1.91)	0.00767
Carcinoid syndrome	64	25397	1.60 (1.13 - 2.27)	0.00813
Alteration of consciousness	1286	23431	0.89 (0.82 - 0.97)	0.00866
Orthostatic hypotension	412	24101	0.82 (0.70 - 0.95)	0.00877
Postablative ovarian failure	33	25397	0.43 (0.23 - 0.81)	0.00900
Acquired hypothyroidism	189	22973	1.32 (1.07 - 1.62)	0.00902
Other disorders of metabolism	260	28417	1.27 (1.06 - 1.51)	0.00933
Anxiety, phobic and dissociative disorders	3414	19702	0.93 (0.88 - 0.98)	0.00954
Allergic conjunctivitis	416	25181	0.82 (0.71 - 0.95)	0.00970

Supplemental Table 13: Regular expressions to find bundle branch blocks within ECG impressions. At Vanderbilt, these impressions are largely typed, and thus contain frequent abbreviations. All searches were performed insensitive to case.

Phenotype	Definition in ECG Reports
LBBB	'LBBB|left bundle branch block|left BBB'
RBBB	'RBBB|right bundle branch block|right BBB'
LPFB	'LPFB|left posterior fascicular block|left PFB'
LAFB	'LAFB|Left anterior fascicular block|left AFB'
BBB	Records matching either the LBBB or RBBB regular expressions.

Supplemental Table 14: Associations from electrocardiogram phenotypes from BioVU. There were 2106 African ancestry (AA) controls and 15432 European ancestry (EA) controls.

Phenotype	Population	Cases	Odds Ratio (95% CI)	p
BBB	AA	278	1.28 (1.02 - 1.62)	0.035
LAFB	AA	218	1.34 (1.04 - 1.72)	0.023
LBBB	AA	91	1.54 (1.05 - 2.25)	0.026
LPFB	AA	48	1.31 (0.79 - 2.17)	0.296
RBBB	AA	195	1.25 (0.96 - 1.63)	0.103
BBB	EA	2876	0.96 (0.90 - 1.03)	0.231
LAFB	EA	1870	0.92 (0.86 - 1.00)	0.038
LBBB	EA	983	0.90 (0.81 - 1.00)	0.051
LPFB	EA	400	1.00 (0.85 - 1.16)	0.949
RBBB	EA	2001	0.99 (0.92 - 1.06)	0.752